J Mater Sci (2011) 46:6964–6974
DOI 10.1007/s10853-011-5664-8

Effects of Al_2O_3 particle reinforcement on the lubricated sliding wear behavior of ZA-27 alloy composites

Miroslav Babic · Slobodan Mitrović · Fatima Zivic

Received: 4 March 2011 / Accepted: 26 May 2011 / Published online: 4 June 2011

Abstract The present investigation deals with the effect of Al_2O_3 particle reinforcement on the lubricated sliding behavior of ZA-27 alloy. The composites with 3, 5, and 10 wt% of Al_2O_3 particles were produced by the compocasting procedure. Tribological properties of alloy and composites were studied, using block-on-disk tribometer at different specific loads and sliding speeds. The test results revealed that composite specimens exhibited significantly lower wear rate, but higher coefficient of friction than the matrix alloy specimens in all the combinations of applied loads and sliding speeds. The improved antiwear characteristics of the composites were influenced by positive effects of higher frictional heating on compatibility of the composite phases and suppressing micro-cracking tendency. Due to that, effects of reinforcing hard particles were manifested through the reduced wear rate of composites, especially in conditions of higher load, lower sliding speeds and higher Al_2O_3 particle content. In present wear tests, the significant forming of mechanically mixed layers was not noticed, what is confirmed by the SEM microphotographs.

Introduction

Over the past few decades Zinc-Aluminum alloys (ZA alloys) have been widely investigated as promising material for tribological applications. At this moment the ZA alloys have become the alternative material primarily for aluminum cast alloys and bearing bronzes due to good castability and unique combination of properties [1–11]. They can also be considered as competing materials for cast iron, plastics, and even steel when being applied for operation under conditions of high mechanical loads and moderate sliding speeds (moderate operation temperatures) [12, 13]. Interest for extending the practical application of these alloys is based on tribological, economic, and ecological reasons [14–17].

Major limitations of the ZA alloys are their inferior elevated temperature mechanical and wear properties, dimensional instability at temperatures above 120 °C and large coefficient of thermal expansion [9]. One of the possible measures for overcoming these deficiencies is reinforcement of the ZA alloy by incorporation of thermally stable second phase [1, 10, 11] to form composites. This approach is based on positive experiences about the influence of the ceramic particle reinforcement on properties of aluminum-based alloys.

Mechanical properties' characterization of ZA alloys reinforced with dispersed hard ceramic particles has been a matter of broad interest over the recent years. It was reported that hard and thermally stable ceramic reinforcements in ZA alloys contributed to a higher hardness [10–14], superior elastic modulus [12], and lower coefficient of thermal expansion of the matrix alloy at ambient temperature [15]. Furthermore, increasing content of reinforcing phase leads to further improvement of properties. The increase of hardness could be accompanied with decrease of strength [11, 12] or without this effect [13]. However, composites attain improved elevated temperature strength [13].

The tribological characteristics of ZA-based metal matrix composites (MMCs) have received little attention. The primary attention has been focused on ZA alloy

M. Babic (✉) · S. Mitrović · F. Zivic
Faculty of Mechanical Engineering, Tribology Center, University of Kragujevac, Sestre Janjic 6, 34000 Kragujevac, Serbia
e-mail: babic@kg.ac.rs

reinforced by SiC particle. Generally, the presence of hard ceramic particles contributes to an improvement of resistance to abrasion [9, 16, 17] and erosion/corrosion [18, 19] of MMCs based on ZA alloys matrix. However, the effectiveness of particles influence depends on the dominance of set factors, such as: subsurface hardening, micro-cracking tendency, damage of reinforcement, removal of the reinforcement phase [20].

Sharma et al. [21] investigated the tribological effect of silicon carbide (SiC) reinforcement on the unlubricated sliding wear behavior of ZA-27 alloy composites using a pin-on-disc sliding wear testing machine. They revealed that the composites exhibited a lower wear rate compared to the unreinforced alloy specimens in conditions of dry sliding. Reduced wear rate of ZA-27/SiC composite in lubricated sliding conditions was also reported by Tjong and Chen [22]. The addition of the SiC particles of various sizes to the ZA-27 alloy led to a wear response improvement at all normal loads. However, positive influence was significant only with 5 vol.% of SiC content.

The positive effect of the addition of SiC particles on improvement of the wear resistance of ZA-27 alloy in conditions of dry and lubricated sliding was confirmed by research of Auras and Schvezov [23]. Besides the ZA-27/SiC composites, ZA-37/SiC composites were studied, too. Prasad [24] analyzed the dry sliding wear response of a ZA-37 alloy reinforced with 10 wt% SiC particles over a range of applied pressures (prior to seizure) at the sliding speeds 1.26 and 2.52 m/s. Incorporation of dispersoid (SiC) particles improved the wear resistance and seizure pressure of the ZA-37 matrix alloy. Frictional heating reduced in the case of the composite as compared to that of the matrix alloy. Further, presence of the reinforced (SiC) particles increased the seizure temperature of the matrix alloy. The same author [10] reported that the reinforcement of ZA alloys by the silicon carbide particles led to a reduction of the wear rate of the alloy in oil lubricated conditions. The positive effects on tribological behavior of ZA alloy were also obtained with zirconium particles [25], garnet particles [26], and short glass fibers [27].

Very limited effort has been made to understand the influence of Al_2O_3 particles on the sliding wear behavior of ZA alloys. The dry sliding wear behavior of ZA alloy reinforced by Al_2O_3 particle is influenced by the sliding speed and pressure [11]. At low sliding speed, significantly lower wear rate of the matrix alloy over that of the composite was noticed. Reduced wear rate and higher seizure pressure experienced by the composite over that of the matrix alloy at the higher sliding speeds. The results of our dry wear tests [28] revealed that ZA-27/SiC composite specimens exhibited significantly lower wear rate than the matrix alloy specimens in all combinations of applied loads and sliding speeds. The difference in the wear resistance of composite with respect to the matrix alloy, increased with the increase of the applied load/sliding speed.

The higher [11] or slightly lower [28] wear rate level of composites than that of the matrix alloys in conditions of lower sliding speeds was attributed to the predominant effect of micro-cracking tendency of composites. Suppressing micro-cracking tendency at higher sliding speeds/loads has resulted in increase of the tribological superiority of composites with respect to the matrix alloy. The difference in the wear resistance of the composite with respect to the matrix alloy, increased with the increase of Al_2O_3 particle content [28].

The majority of the available results of tribological behavior of ZA alloys reinforced by Al_2O_3 particles pertain to dry sliding conditions. However, for sliding contacts where high friction and wear are undesirable the use of a lubricant is necessary. In view of the above, in this study an attempt has been made to analyze the lubricated sliding wear behavior of a ZA-27 alloy reinforced by Al_2O_3 particles. The influence of changing concentration of Al_2O_3 in composite samples has been examined under varying applied pressure and sliding speed. The matrix alloy has also been tested in identical conditions to understand the role played by the Al_2O_3 particles in influencing the behavior of the matrix alloy. The observed wear response of the samples has been substantiated through the wear rate and morphology of the worn surfaces.

Experimental

Preparation of the composites

The ZA-27 alloy, with the chemical composition shown in Table 1, was processed by the liquid metallurgy route. The purity of aluminum was 99.90%, zinc 99.99%, and copper 99.5%. Alloy was melted in a graphite crucible in an electric resistance furnace. The melt was overheated to 680 °C and cast into a steel mold to obtain samples as 100 mm long bars with rectangular cross-section with dimensions of 30 × 20 mm^2. No grain refinement treatment was performed during the process of casting. The Al_2O_3 particles of mean size of 220 μm with contents of 3, 5 and 10 wt% were used as reinforcement.

The composite was synthesized by dispersing alumina particles in the ZA-27 alloy matrix using compocasting

Table 1 Chemical composition (wt%) of ZA-27 alloy

Element	Al	Cu	Mg	Fe	Zn
Percentage	28.47	2.51	0.011	0.145	Balance

isothermal technique, detailed elsewhere [8, 28], but summarized as follows. The process consists of melting ZA-27 chemically cleaned bars, heating of the melt above the alloy melting point (for additional cleaning of the slag), cooling down and ''mixing in'' of the Al_2O_3 particles into the semi-solidified melt of ZA-27 at the temperature of 462 °C. No chemical pretreatment of Al_2O_3 was performed except that the powder was preheated to 462 °C to avoid the disturbance of isothermal condition in the melt during the compo casting process. After the mixing of the composite was finished, the mass was cooled down to 430 °C and it was poured into the steel mold, which was previously heated up to 300 °C. Cylindrical bars were obtained with 36 mm diameter and length of 100–130 mm. After obtaining the composite materials samples, it was necessary to perform the hot pressing to reduce porosity. The samples for the tribological investigations were then made from the ZA-27 as-cast alloy and pressed composite pieces.

Microstructural and mechanical characterization

Microstructural and mechanical characterization of matrix material and composites included metallographic examinations with optical microscope (OM) and micro-hardness measurements. Metallographic samples were prepared in a standard way applying grinding and polishing, whereas etching in Keller's solution (the mixture of 95 mL H_2O, 2.5 mL HNO_3, 1.5 mL HCl, and 1 mL HF) was used to reveal the microstructure. Micro-hardness of the specimens was measured using a Vickers hardness tester at an applied load of 0.3 kg. At least six measurements were made for each specimen in order to eliminate possible segregation effects and to get a representative value of the material hardness. Density of the specimens was measured by Archimedes method.

Sliding wear tests

The specimens were tested using a computer aided block-on-disk sliding wear testing machine with the contact pair geometry in accordance with ASTM G 77-98. A schematic configuration of the test machine is shown in Fig. 1. More detailed description of the tribometer is available elsewhere [29].

The test blocks (6.35 × 15.75 × 10.16 mm) were prepared from the Al_2O_3 reinforced ZA-27 alloy composite and as-cast ZA-27 alloy. Their contact surfaces were polished to a roughness level of $R_a = 0.2$ μm. The counter face (disk with 35 mm diameter and 6.35 mm thickness) was fabricated using the casehardened 30CrNiMo8 steel with hardness of 55 HRC. The roughness of the ground contact surfaces was $R_a = 0.3$ μm. The tests were performed under lubricated sliding conditions at different sliding speeds (0.26–1.00 m/s) and normal loads (10–80 N), with a sliding distance of 1000 m. Each experiment was repeated five times.

The tests were performed at room temperature. The lubricant used was ISO grade VG 46 hydraulic oil, a multipurpose lubricant recommended for industrial use in plain and antifriction bearings, electric motor bearings, machine tools, chains, and gear boxes, as well as in high-pressure hydraulic systems. During the tests the disks were continuously immersed up to 3 mm of depth in 30 mL of lubricant.

The wear behavior of the block was monitored in terms of the wear scar width (Fig. 1). Using the wear scar width and geometry of the contact pair, the wear volume (in accordance with ASTM G77-83) and wear rate (expressed in mm^3/m) were calculated. The friction coefficient was obtained automatically during the tests by means of data acquisition software.

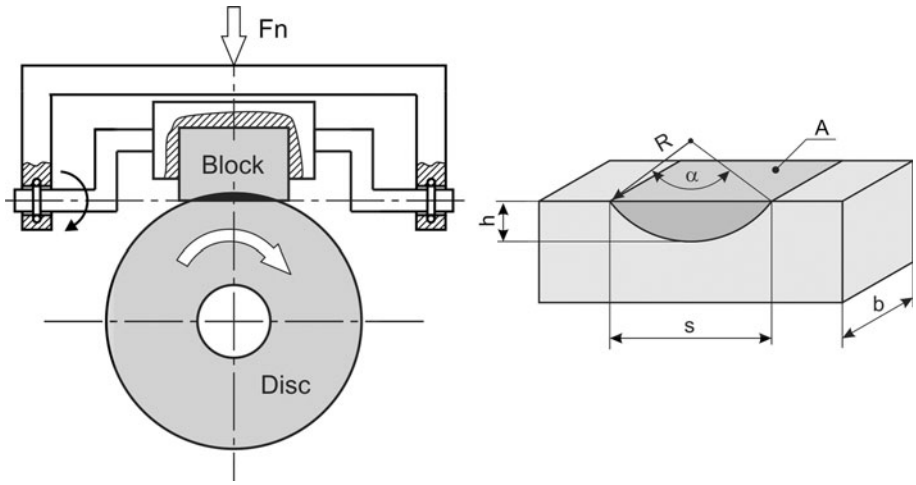

Fig. 1 The scheme of contact pair geometry

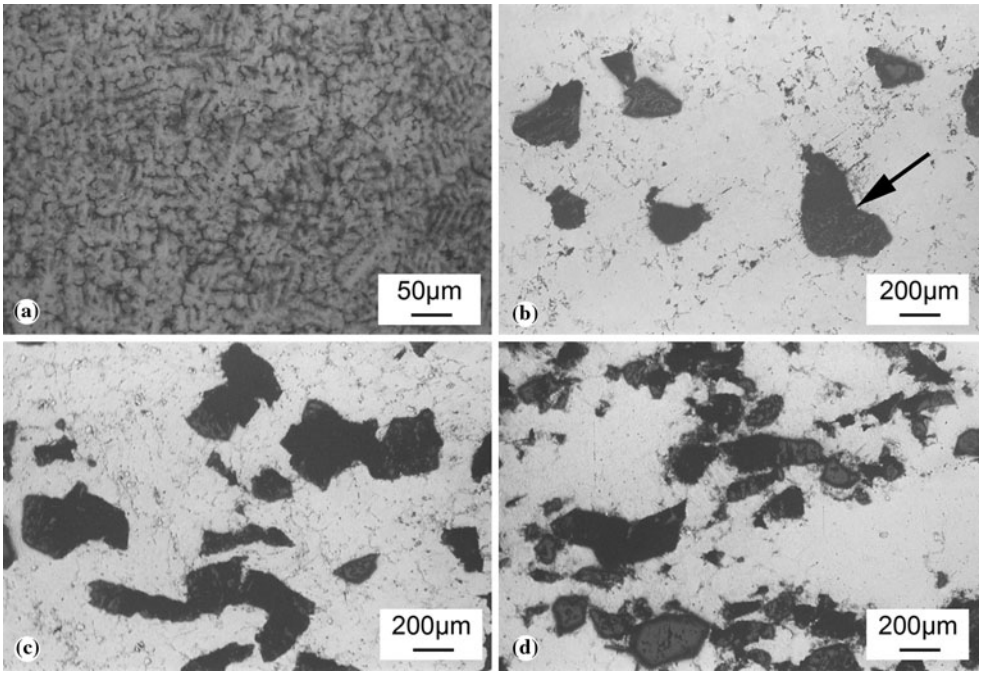

Fig. 2 Microstructure of the tested materials: **a** ZA-27 alloy, **b** composite 3% Al_2O_3, **c** composite 5% Al_2O_3, and **d** composite 10% Al_2O_3

Results and discussion

Microstructure, hardness, and density

The typical OM micrographs of the matrix alloy and composite are shown in Fig. 2. The microstructure of the matrix alloy revealed primary α dendrites and eutectoid $\alpha + \eta$ phase (Fig. 2a). In order to establish the distribution of the Al_2O_3 particles in alloy matrix volume, some of the samples were cut in the middle, perpendicular to the surface which has the role of the contact surface in tribological test. The microstructure was observed both on the contact surface and along the sample's depth, i.e., on the surface of the cross-section. The typical micrographs (Fig. 2b–d) point to the relatively uniform distribution of the Al_2O_3 second phase for all of the three contents (3, 5, and 10 wt%). The dispersoid/matrix interfacial bonding was observed to be reasonably sound (Fig. 2b, c, region marked by an arrow).

The distribution of the reinforcing particles points to a tendency that a lot of particles are placed in the inter dendritic phase area. This is clear due to mixing of the semi-solidified melt of the alloy, which, at the process temperature, contains a large portion of the liquid phase and low resistance to the infiltration of particles. Later, during the cooling, the particles became rounded. It is interesting that there is a large number of particles that are placed within the primary dendrites, what points to their relatively large energy acquired from the mixer. It looks like a ''knocking-in'' of the particles into the dendrites.

Table 2 Hardness and density of matrix alloy and composites

Properties	ZA-27	Composites		
		3% Al_2O_3	5% Al_2O_3	10% Al_2O_3
Hardness ($HV_{0.3}$)	103	106	109	113
Density (g/cm^3)	4.85	4.36	4.14	3.73

The results of hardness and density measurements are shown in Table 2. From Table 2 it can be seen that the hardness of tested materials increases with addition of Al_2O_3 particles. Density decrease with addition of Al_2O_3 particles.

Tribological tests

Figure 3 shows wear curves of tested specimens at sliding speed of 0.26 m/s and applied load of 80 N. The presented shape of curves is typical also for the other combinations of sliding speed and applied load. Generally, the wear behavior of tested materials was characterized by initially very intensive wear (run-in) during the first minutes of sliding, after which the steady-state period followed. Intensive initial wear is a consequence of the nominal line contact Hertzian geometry for the contact pair, namely the very large real contact loads. The real contact surface increases with wear increase, what causes rapid drop of the contact pressure. Besides that, the lubricating conditions are improving with forming of the worn surface, what also contributes to entering into the steady-state regime of wear.

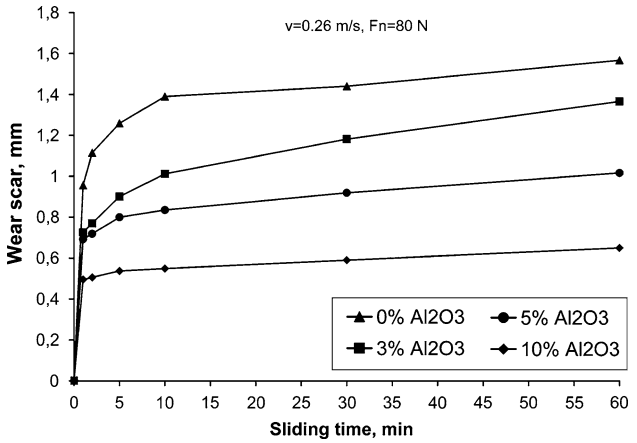

Fig. 3 Wear curves of tested materials at sliding speed of 0.26 m/s and applied load of 80 N

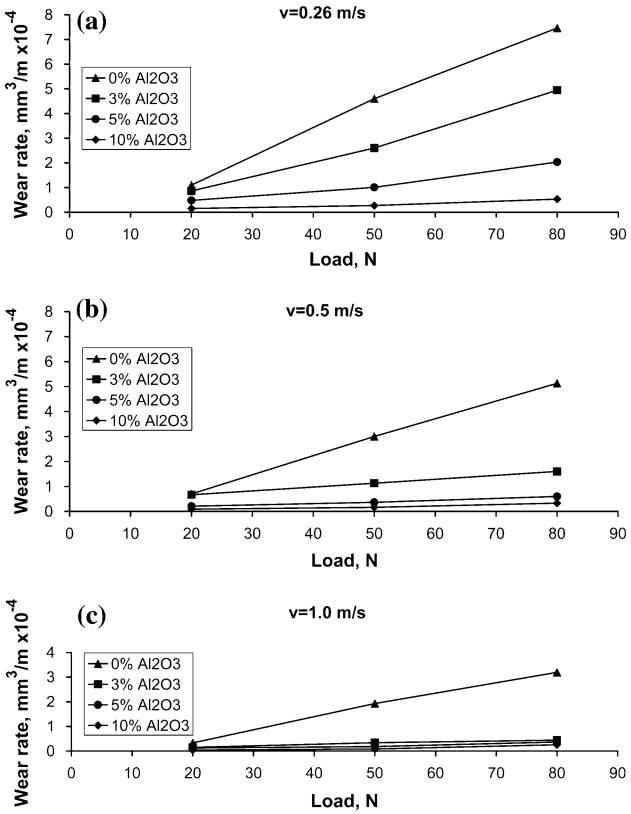

Fig. 4 Wear rate vs. applied load of the ZA-27 alloy composites at different sliding speeds: **a** 0.26 m/s, **b** 0.5 m/s, and **c** 1.0 m/s

It is noticeable that the period of initial wear is getting shorter with increase of the mass share of the reinforcers. That can be explained by the fact that in samples which have the largest share of the reinforcers, the real contact is realized over the larger number of the Al_2O_3 particles which play the role of the load carriers. It could be noticed that the wear of composites containing particles was always significantly lower when compared to the matrix ZA-27 alloy.

Figure 4 shows the wear rate of the tested materials as a function of applied load at different sliding speeds. The graphs indicate that the wear rate of the matrix alloy, as well as that of the composite, increase with applied load at all tested sliding speeds. The graphs are almost linear (especially at the higher sliding speeds). Generally, the slope of curves decreases with increase of the percentage share of the reinforcer. Dependence of the wear rate on the load in case of matrix alloy was approximately linear at all levels of sliding speed.

Figure 5 shows the effect of sliding speed on the wear rate of the tested materials at different applied loads. The wear rate of both, the unreinforced alloy and composite specimens, decreases with increase in the sliding speed. The decreasing trend of the wear rate was observed much more distinctive at the lower level of sliding speed and higher level of applied load. Variation of slope of the wear rate vs. sliding speed of composites curves occurred at transition sliding speed of 0.5 m/s.

Also, from Figs. 4 and 5 it can be clearly seen that sensitivity of composites to variation of the normal load and sliding speed decreases with the increase of the Al_2O_3 reinforcing particles content. The graphs also suggest that composite specimens exhibited significantly lower wear rate than the matrix alloy specimens in all combinations of applied loads and sliding. The difference in the wear resistance of composites with respect to the matrix alloy increased with the increase of applied load and decrease of the sliding speed. Generally, positive effects of reinforcing of ZA-27 alloy increases with increase of the percentage content of the Al_2O_3 particles, what is shown in Fig. 6 by diagrams of the wear rate decrease with increase of the Al_2O_3 content.

The variation of the friction coefficient during sliding is illustrated in Fig. 7. This is a graphical representation of the results obtained for applied load of 50 N at different sliding speeds. The graphs show that significantly higher friction coefficient corresponds to the composite as compared to the matrix, at all sliding speeds. Besides that, the different nature of the friction coefficient was noticed during the run-in period. In the case of the matrix alloy, during the first few minutes intensive run-in of the contact surfaces is occurring, accompanied by the fast drop of the friction coefficient. On the contrary, in the case of composite specimens, the coefficient of friction initially increased with test duration at high rate, followed by a low rate of decrease for longer test duration.

Figure 8 shows the steady-state coefficient of friction of the tested materials as a function of applied load at different sliding speeds. The graphs indicate that the coefficient of friction of the matrix alloy, as well as that of the

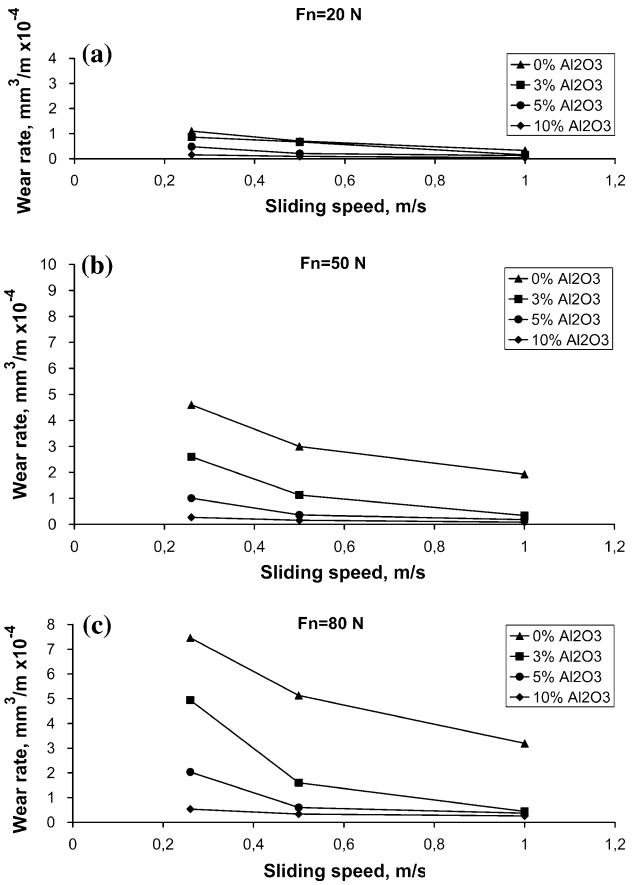

Fig. 5 Wear rate vs. sliding speed of the ZA-27 alloy composites at different applied loads: **a** 10 N, **b** 50 N, and **c** 80 N

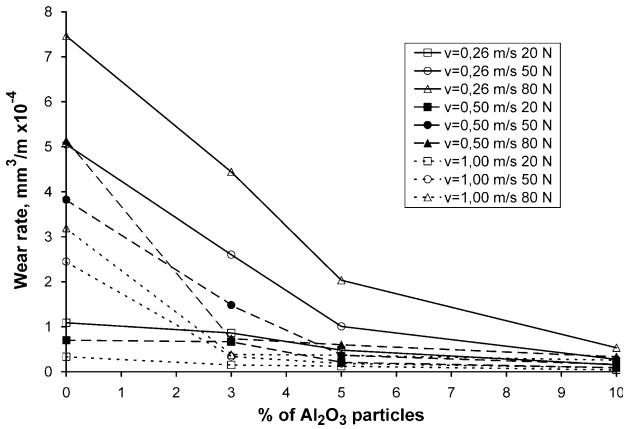

Fig. 6 Wear rate vs. wt% of Al_2O_3 reinforced ZA-27 alloy composites at various sliding speeds and loads

composite, increases with applied load at all sliding speeds and they are almost linear.

The dependence of the steady-state friction coefficient on the sliding speed, for various normal forces is shown in Fig. 9. The friction coefficient decreased with increase of the sliding speed. Decreasing of the friction coefficient is

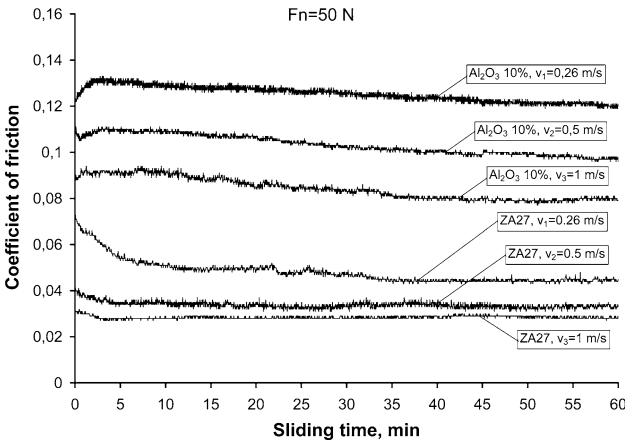

Fig. 7 Friction coefficient variation of tested materials during sliding time at load of 50 N and different sliding speeds

especially prominent in a region of lower sliding speeds. Decrease of the friction coefficient in lubricated tests with increase of the sliding speed and decrease of the applied load (i.e., with increase of the v/F_n ratio), as well as the obtained range of the friction coefficient (from 0.04 to 0.13), point to the fact that the friction was occurring in regimes of boundary lubrication. In conditions of the lowest applied load and the highest sliding speed, friction was occurring in regime of transition from boundary to mixed lubrication.

The graphs in Figs. 7, 8, and 9 suggest that composite specimens exhibited significantly higher coefficient of friction than the matrix alloy specimens in all combinations of applied loads and sliding. Generally, friction properties are worsening with increase of the percentage content of the Al_2O_3 particles.

Figure 10 represents typical worn surfaces of the samples. The worn surfaces of matrix alloy showed the relatively deep parallel grooves in direction of sliding (Fig. 10a, region marked by G), scratches (S), damages, and smeared material (T). In addition, the scanning electron micrograph exhibits moderate appearance of the surface fatigue damages after repeated unidirectional sliding of block over the disc (C).

The worn surfaces of composite samples were noticed to be smoother than those of the as-cast one (Fig. 10b vs. a). A relatively clean surface is marked by shallow grooves what indicates the low wear loss. On the shown portion of the worn surface one can observe hard reinforcement Al_2O_3 particles which are exposed and offer resistance to the softer matrix against wear (Fig. 10b, particle marked by P_1 and clustered region of smaller particles marked by P_2). Besides that, the hard reinforcement Al_2O_3 particle can be seen, lying immediately beneath the contact surface (marked by P_3), that will be exposed during process of wear.

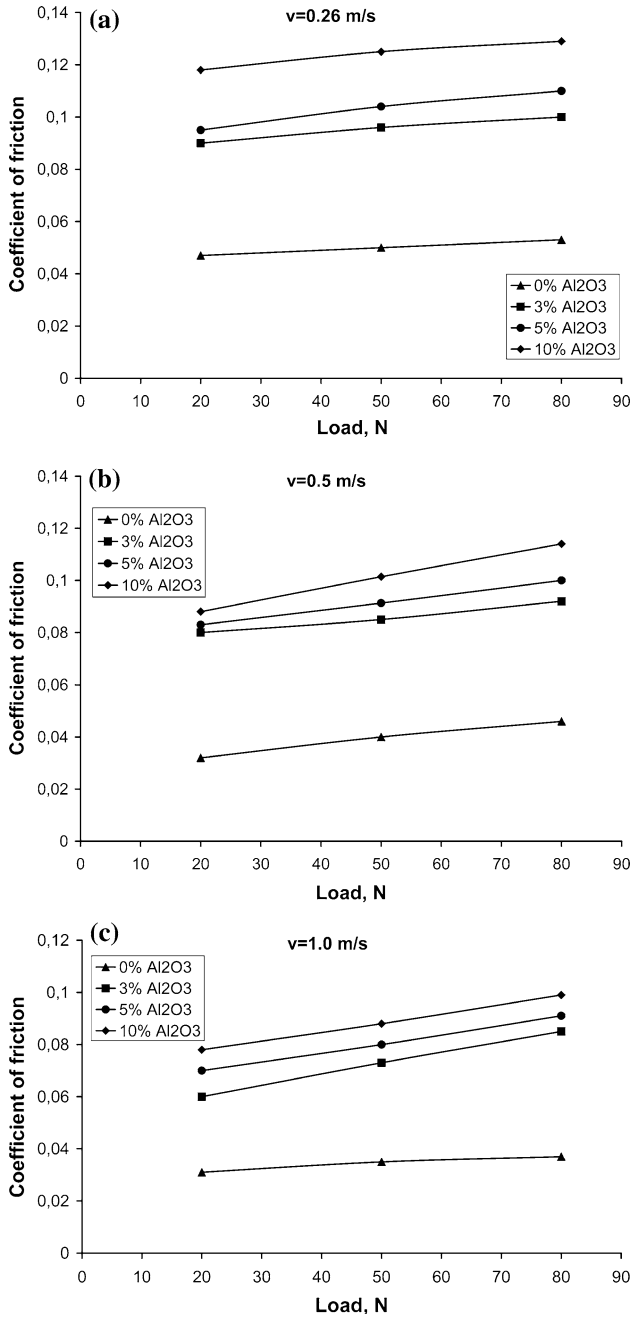

Fig. 8 Coefficient of friction vs. applied load of the ZA-27 alloy composites at different sliding speeds: **a** 0.26 m/s, **b** 0.5 m/s, and **c** 1.0 m/s

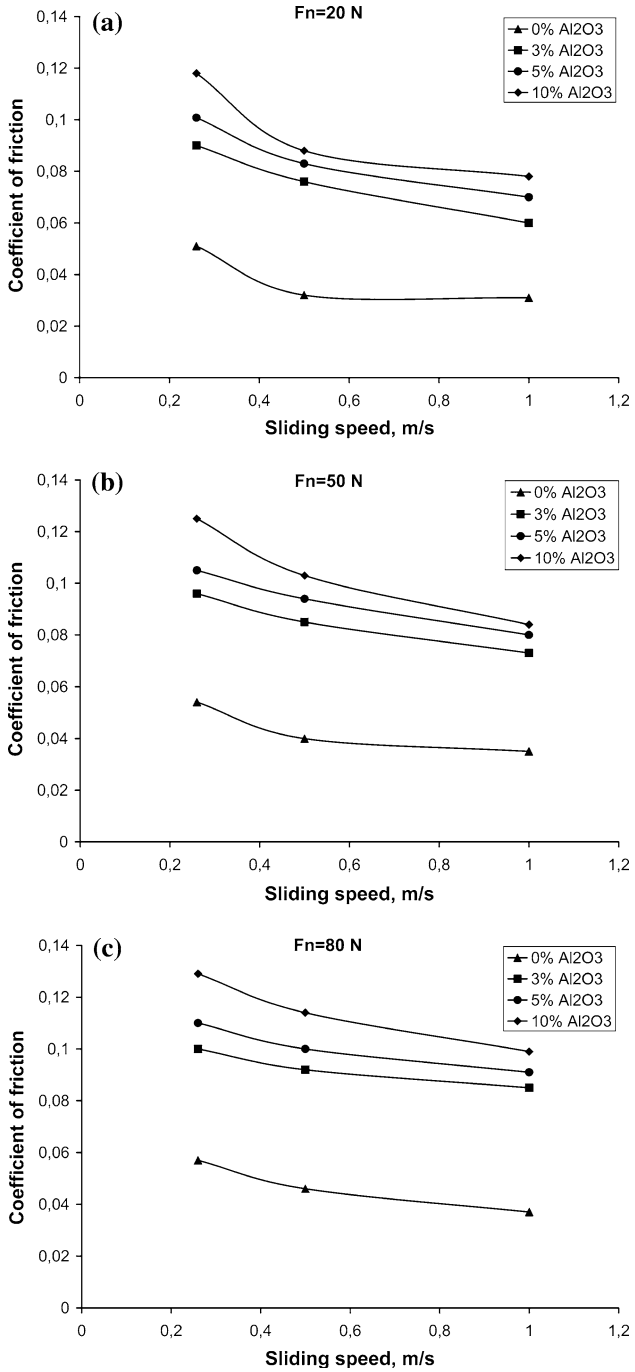

Fig. 9 Coefficient of friction vs. sliding speed, during lubricated sliding, of the ZA-27 alloy composites at applied load of **a** 20 N, **b** 50 N, and **c** 80 N

On the worn surface of composites one can also notice appearance of the brittle fractures (Fig. 10c). Namely, during sliding, the nucleation and propagation of cracks within Al_2O_3 particles and matrix alloy occurred causing the brittle fracture. In the region around the wear scar edges, clearly visible are evenly distributed Al_2O_3 particles, debonded, sheared and then adhered to the surface (Fig. 10d, marked by arrow).

Discussion

Generally, the obtained results suggest that composite specimens exhibited significantly lower wear rate than the ZA-27 matrix alloy specimens in all combinations of applied loads and sliding speeds in lubricated sliding conditions. Superior wear characteristics of ZA-27 alloy

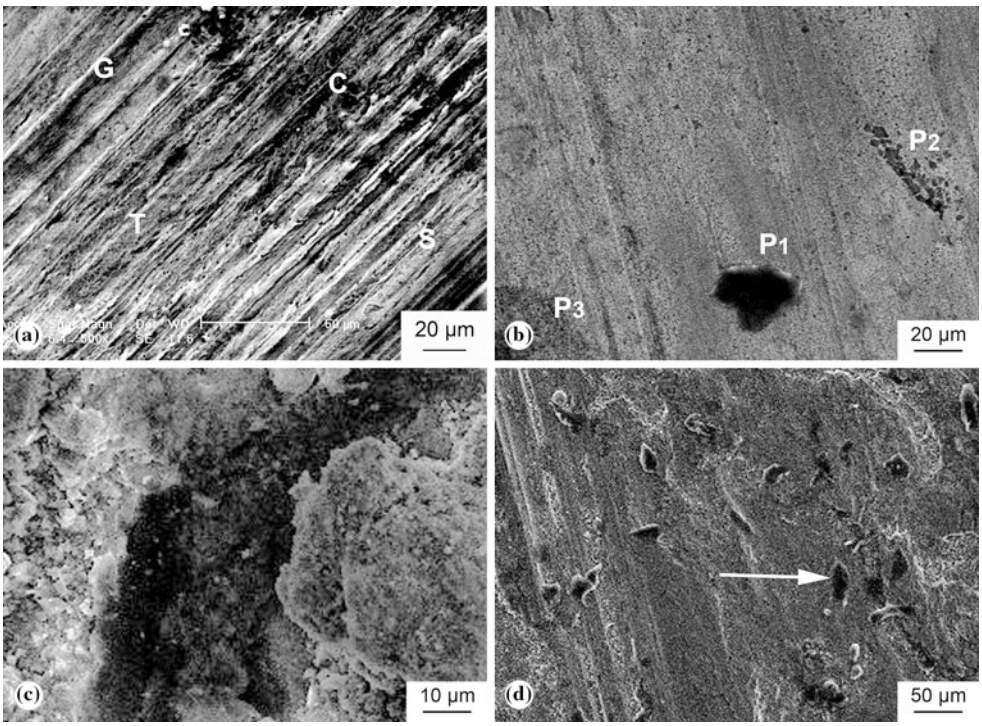

Fig. 10 SEM micrographs of worn surfaces: **a** ZA-27 alloy, **b–d**) 5% Al_2O_3 reinforced composite sample (sliding speed of 0.5 m/s and applied load of 80 N)

reinforced by Al_2O_3 particulate in conditions of dry sliding and lubricated sliding, especially at higher sliding speeds and pressures, have also been reported by investigators [11, 28]. As opposite to the positive effect on the antiwear properties, adding of Al_2O_3 particles to ZA-27 alloy caused increase of coefficient of friction. Same nature of ceramic particulate reinforcement effects on frictional behavior of zinc-based alloy (ZA-37) reported Prasad [10].

The increased level of friction coefficient of composites over that of the matrix alloy could be attributed to two-body and three-body abrasive action caused by hard particles of reinforcement. Namely, during the run-in process of intensive sliding wear of matrix material, hard particles protrude on the composite contact surface causing roughness to be higher [10]. This phenomenon of exposed Al_2O_3 particles as well as entire cluster of smaller particles can be clearly spotted on the microphotograph in Fig. 10b. These protruded particles bear contact loads and protect the alloy material from direct contact with the steel counter surface. However, they cause very intensive plowing of the counter face material and increase of the friction coefficient. Also, during the wear process, fractured and liberated particles lead to phenomenon of the three-body abrasive process, particularly of the counter face material. The friction coefficient is a function of three mechanisms: asperity deformation, adhesion, and plowing of the interface by hard asperities and particles [30]. The total friction coefficient is the weighted sum of these three components, depending on the local friction condition that prevails at the sliding interface.

Specifics of the friction process caused by adding the reinforcement particles to matrix alloy can be clearly noticed on graphs that show dependence of the friction coefficient on the sliding time (Fig. 7). Diagrams that are related to the matrix alloy have clearly prominent run-in period during which the friction coefficient drop occurs. That is in accordance with the process of intensive initial wear in conditions of initial nominal Hertzian line contact. Namely, in that conditions (Fig. 1), Hertzian contact stresses were extremely high as a result of non-conformal surfaces, which would preclude any lubrication regime other than boundary [29, 31]. Appearance of initial friction coefficient drop is especially emphasized in conditions of smaller sliding speeds and higher applied loads, i.e., in conditions of strong boundary lubrication. However, as the test proceeded, wear resulted in conformal contact surfaces (Fig. 7) and a substantial drop in friction coefficient, a pattern consistent with a transition from boundary to mixed lubrication conditions in which the friction coefficient has almost steady level.

On the contrary, in case of composite specimens the coefficient of friction increased with test duration at high rate initially, followed by a low rate of decrease at longer test duration. In composites, at the very beginning, the

intensive wear contributes to increase of the number of contacts of the hard abrasive Al_2O_3 particles with the counter face material, what is manifested through increase of the friction coefficient and slower wear of composites, with respect to the matrix material. The small initial wear contributes to slower increase of the conformal contact surface, what is accompanied by a very moderate drop of the friction coefficient level during the steady-state process.

Tribological behavior of the ZA-27 was well investigated. Zn–Al based alloys basically comprise a mixture of the two solid solutions of α and γ phases, which impart load bearing and solid lubricating properties [21, 25, 28]. Effects of these micro constituents on tribological behavior of the alloy depend on their distribution, size, and operating temperatures. The incorporation of the Al_2O_3 particulate reinforcement led to a reduction in the lubricated sliding wear rate of ZA-27 alloy. Generally, the hard phase provides protection of the alloy matrix and offers increased load bearing capacity that leads to less wear in composite as compared to the matrix alloy. However, the effectiveness of particles influence on tribological behavior of the composite can be degraded due to the cracking tendency and removal of the reinforcement phase. Those phenomena can be clearly seen on the SEM photographs of worn surfaces of composites in Fig. 10c and d. The just described higher level of the friction coefficient with respect to the matrix alloy, established in composites, has the key role in preventing the undesired micro-cracking tendencies caused by Al_2O_3 reinforcing particles. Namely, predominant micro-cracking tendency appears at lower operating temperatures, i.e., in conditions of lower level of friction. This is a consequence of poor compatibility between the hard dispersoid phase and the matrix alloy [12, 17, 28, 29, 32].

Increased friction contributes to compatibility of the composite phases, suppressing micro-cracking tendency. In conditions of higher frictional temperatures the matrix acquires some viscoplasticity into contact layers. It provides softer and ductile matrix to be more accommodative, supporting the dispersoid particles in position [23, 24, 28]. Accordingly, suppressing micro-cracking tendency, the dispersoid phase allows a more effective transfer of load between matrix and dispersoid phase and effective carrying of load. Due to that, effects of reinforcing hard particles are manifested through the reduced wear rate and higher seizure pressure of the composite over that of the matrix alloy at high sliding speeds and loads. Although the obtained results suggest that the composite specimens exhibited significantly lower wear rate than the ZA-27 matrix alloy specimens, the degree of reduction depends on the applied loads and sliding speeds. At the lowest applied load of 20 N and the highest sliding speed of 1.00 m/s the confirmed differences are very moderate (Fig. 5a). In such contact conditions, the mixed lubrication is realized with the lowest friction coefficient, namely, the lowest friction temperature is generated, what is caused by the influence of micro-cracking tendency on the wear of composite. With increase of the v/F_n ratio, the transition into the regime of boundary lubrication with increase of the friction coefficient is realized, as well as increase of local friction temperatures resulting in improvement of the compatibility between the hard dispersoid phase and the matrix alloy. In accordance with such a nature of the contact conditions influence on friction behavior of tested samples, the difference in the wear rate level of composites, with respect to the matrix alloy, increases with increase of the contact load and decrease of the sliding speed. The same nature of influence of the contact load was confirmed in the dry sliding conditions [28]. However, the influence of the sliding speed is quite opposite, what is in accordance with influence on the contact temperature.

Obtained results also point to the fact that in all the combinations of the contact load and sliding speeds, the antiwear improvement of ZA-27 alloy increases with increase of the percentage content of the Al_2O_3 particles (Fig. 6). The wear rate reduction is the largest at the Al_2O_3 particles content change from 0 to 3%, or from 0 to 5%, depending on the contact conditions. Diagrams with the rapid drop of the wear rate with variation of the Al_2O_3 particles content correspond to conditions of the lower sliding speeds, all the way up to 5%, with the slopes of the curves significantly smaller after that. In conditions of the highest sliding speed of 1.0 m/s, a very prominent drop of wear rate with increase of the Al_2O_3 particles content up to 3% is noticed. Influence of the further increase of Al_2O_3 content is shown through the moderate influence on the composites' wear rate decrease. Such an influence is in accordance with the described influence of the sliding speed on the frictional behavior of the tested materials. Namely, at conformal contact geometry, which is created after the intensive run-in wear conditions at the high sliding speed, the conditions are created for the mixed lubrication, where the mating surfaces are separated with a significantly thick fluid film and where the influence of the contact materials characteristics on the tribological processes is decreasing.

Generally, tribological behavior of composites with hard second phase like Al_2O_3, could be a result of very complex mechanisms involved in a wear caused by micro-cracking tendency, as well as generation and destruction of mechanically mixed layers (MMLs) on the mating surfaces [28, 33]. Namely, formation of wear debris, fragmentation of oxide layer, transfer of materials between the contact surfaces and mixing and compaction of these constituents mechanically on the surfaces under applied load and higher frictional heating, lead to formation of MML during sliding

wear of metals and alloys. The phenomenon of the MML creation is especially prominent in contact of alloys reinforced by ceramic particles and steel [28]. Hard ceramic particles are significantly harder than the counter steel surface and scratch the counter surface materials. That causes generation of more counter surface debris (steel particles) that gets compacted on the specimen surfaces during sliding wear process. Additionally, the possibility of accumulation of wear debris at the valleys between the protruded ceramic particles is greater in composite as compared to the alloy. The formation of mechanically mixed layers was observed in similar investigation in conditions of dry sliding [28]. Creation and destruction of those tribo-induced layers within the contact zone controlled the process of wear. However, in present wear tests the significant forming of mechanically mixed layers was not noticed, what is confirmed by the SEM microphotographs shown in Fig. 10. Such results are also reported by Auras and Schvezov [23]. In that study ZA-27 alloy reinforced by SiC particles showed the lowest wear rate. Also, iron transfer was found only for the ZA-27 alloys. The presence of an MML was not found in the other alloys. The small appearance of the MMLs is a consequence of the lubricating oil circulation through the contact zone (disc's peripheral area was immersed in the lubricating oil). The lubricating oil provides the moving of the debris and its removing from the contact zone, what decreases chances for their compaction and sintering. On the microphotograph in Fig. 10d one can notice defragmented Al_2O_3 particles concentrated in the exit contact zone. By the constant rotation of disc periphery trough oil, the unsettled tiniest fractions of debris are being brought into the contact zone again. Their presence between the contact surfaces prevents the inter-metallic contact, what is resulting in a low wear rate [34].

The predominant wear mechanism of tested ZA-27 alloy was the mild wear of plastically deformed surface by micro-plowing, scratching, and adhesion. The grooves and scratches on worn surface of ZA-27 alloy (Fig. 10a) resulted from the plowing action of asperities on the counter disc of significantly higher hardness, as well as due to the hard wear debris. Besides the abrasive wear mechanism, existence of the material smeared onto the sliding surface (clearly visible in Fig. 10a, marked by T) shows presence of the adhesive wear. This material had been detached from the alloy surface by adhesion to the steel surface. During the sliding, some of transferred material was lost, but some was re-embedded and was smeared over the alloy sample surface. In addition, the scanning electron micrograph shown in Fig. 10a, exhibits moderate appearance of the surface fatigue damages after repeated unidirectional sliding of block over the disc (C). Appearance of plowing shallow grooves and fragmented Al_2O_3 particles (Fig. 10b, d) can be noticed on the worn surface of composites. Also, appearance of extraction of the Al_2O_3 particles caused by the fatigue load (Fig. 10c) was observed. The nucleation and propagation of cracks within Al_2O_3 particles and matrix alloy occurred during sliding, causing the brittle fracture.

Conclusions

1. Addition of Al_2O_3 dispersoid phase to the ZA-27 matrix alloy caused a significant decrease in wear rate. The difference in the wear resistance of composites with respect to the matrix alloy increased with the increase of applied load and decrease of the sliding speed. Generally, antiwear improvement of ZA-27 increases with increase of the percentage content of the Al_2O_3 particles. Decrease of the wear rate with wt% of Al_2O_3 particles did not have the linear character. The highest degree of changes corresponded to change of the Al_2O_3 particles content from 0 to 5 wt% at lower level of sliding speed, namely from 0 to 3 wt% at higher level of sliding speed.
2. The wear behavior of reinforced ZA-27 alloy could be attributed to effects of Al_2O_3 particles as well as contact conditions on coefficient of friction, i.e., friction heating of the contact. The hard Al_2O_3 phase provides protection of the ZA-27 alloy matrix of direct contact and that leads to less wear in composite as compared to the matrix alloy. However, protruded, as well as fractured and liberated particles cause very intensive plowing of the counter face material and increase of the friction coefficient. Coefficient of friction increased with increase of load and decrease of sliding speed (lower level of v/F_n ratio). The higher frictional heating contributes to the increased compatibility of the composite phases, suppressing microcracking tendency. The more effective transfer of load between matrix and dispersoid phase and effective carrying of load are manifested through the reduced wear rate of the composites, especially in conditions of higher load and lower sliding speeds.
3. Though the obtained values of the wear rate vary in a relatively wide range, depending on the percentage share of the Al_2O_3 particles and combinations of the applied load and sliding speed of tests, their level generally indicates processes of mild wear, which appears after some sliding distance (after severe run-in wear). Stable level of the steady-state friction coefficient during the process of sliding, of the tested contact pairs, as well as the morphology of the worn surfaces, also point to this conclusion. The wear mode of ZA-27 alloy was mainly micro-plowing, groove, scratches

and adhesion. In the case of composites, slight micro-plowing grooves and micro-cracking, without significant forming of mechanically mixed layer were mainly observed.

Acknowledgements The results of this paper are realized through the national project TR-35021 financially supported by the Ministry of Science of the Republic of Serbia (Project Coordinator: Prof. Dr. Miroslav Babic).

References

1. Babic M, Mitrovic S, Dzunic D, Jeremic B, Bobic I (2010) Tribol Lett 37:401
2. Rac A, Babic M, Ninkovic R (2001) J Balkan Tribol Assoc 7:234
3. Savaskan T, Murphy S (1984) Wear 98:151
4. Pandey JP, Prasad BK, Yegneswaran AH (1998) Mater Trans JIM 39:1121
5. Abou El-khair MT, Daoud A, Ismail A (2004) Mater Lett 58: 1754
6. Babic M, Ninkovic R (2004) Tribol Ind 26:3
7. Babic M, Mitrovic S, Jeremic B (2010) Tribol Int 43:16
8. Vencl A, Bobić I, Jovanović MT, Babić M, Mitrović S (2008) Tribol Lett 32(3):159
9. Prasad BK (2002) Wear 252(3–4):250
10. Prasad BK (2007) Wear 262:262
11. Modi OP, Rathod S, Prasad BK, Jha AK, Dixit G (2007) Tribol Int 40:1137
12. Zhu HX, Liu SK (1993) Composites 5:437
13. Karni N, Barkay GB, Bamberger M (1994) J Mater Sci Lett 13:541
14. Sahin Y (1998) Wear 223:173
15. Li BJ, Chao CG (1996) Metall Mater Trans 27(3):809
16. Modi OP, Yadav RP, Mondal DP, Dasgupta R, Das S, Yegneswaran AH (2001) J Mater Sci 36:1601. doi:10.1023/A:1017523214073
17. Modi OP, Yadav RP, Prasad BK, Jha AK, Das S, Yegneswaran AH (2001) Wear 249:792
18. Modi OP, Prasad BK, Jha AK (2006) Wear 260:895
19. Prasad BK (2000) Wear 238:151
20. Prasad BK, Modi OP, Khaira HK (2004) Mater Sci Eng A 381:343
21. Sharma SC, Girish BM, Kamath R, Satish BM (1997) Wear 213:33
22. Tjong SC, Chen F (1997) Metall Mater Trans A 28(9):1951
23. Auras R, Schvezov C (2004) Metall Mater Trans A 35a(5):1579
24. Prasad BK (2003) Wear 254:35
25. Sharma SC, Girish BM, Kamath R, Satish BM (1999) Wear 224:89
26. Ranganath G, Sharma SC, Krishna M (2001) Wear 251:1408
27. Sharma SC, Satish BM, Girish BM, Kramath R, Asanumat H (1998) Tribol Int 31(4):183
28. Babic M, Mitrovic S, Zivic F, Bobic I (2010) Tribol Lett 38:337
29. Babic M, Vencl A, Mitrovic S, Bobic I (2009) Tribol Lett 36:125
30. Suh NP, Sin HC (1981) Wear 69:91
31. Walker JC, Rainforth WM, Jones H (2005) Wear 259(1–6):577
32. Straffelini G, Bonollo F, Molinari A, Tiziani A (1997) Wear 211:192
33. Rao RN, Das S, Mondal DP, Dixit G (2010) Tribol Int 43:330
34. Hiratsuka K, Muramoto K (2005) Wear 259(1–6):467